Opto-Electronic Advances

Supplementary information

February 2024, Vol. 7, No. 2

DOI: 10.29026/oea.2024.230184

Tailoring electron vortex beams with customizable intensity patterns by electron diffraction holography

Pengcheng Huo[1†], Ruixuan Yu[1†], Mingze Liu[1], Hui Zhang[1], Yan-qing Lu[1,2*] and Ting Xu[1,2*]

[1]National Laboratory of Solid-State Microstructures and Collaborative Innovation Center of Advanced Microstructures, Nanjing University, Nanjing 210093, China; [2]College of Engineering and Applied Sciences, Key Laboratory of Intelligent Optical Sensing and Manipulation and Jiangsu Key Laboratory of Artificial Functional Materials, Nanjing University, Nanjing 210093, China.

[†]These authors contributed equally to this work.

*Correspondence: YQ Lu, E-mail: yqlu@nju.edu.cn; T Xu, E-mail: xuting@nju.edu.cn

This file includes:

Supplementary information for this paper is available at https://doi.org/10.29026/oea.2024.230184

Section 1: Ray theory for structured electron vortex beam (EVB)

In this work, considering a plane electron wave passing through the phase mask with a phase distribution $\varphi = lf(\theta)$ and a radius R, the generalized Snell's law indicates that the transverse wave vector k and its differentiation dk are directly related to the phase gradient along the azimuth direction as follows,

$$\begin{cases} k = \dfrac{\mathrm{d}\varphi}{r\mathrm{d}\theta} = \dfrac{l}{r} f'(\theta) \\ \mathrm{d}k = \dfrac{\mathrm{d}\phi}{r^2\mathrm{d}\theta} = \dfrac{l}{r^2} f'(\theta)\,\mathrm{d}r \end{cases} . \tag{S1}$$

For electron ray occupying an area $r \cdot \mathrm{d}r \cdot \mathrm{d}\theta$ in real space are diffracted to a region in Fourier space, the corresponding area is given by $k \cdot \mathrm{d}k \cdot \mathrm{d}\phi$, here $\phi = \theta + \pi/2$ is the azimuth angle in Fourier space. Ignoring reflection and absorption, and considering the energy conservation law, we can obtain the following relationship,

$$I \cdot k \cdot \mathrm{d}k \cdot \mathrm{d}\varphi = I_0 \cdot r \cdot \mathrm{d}r \cdot \mathrm{d}\theta\ , \tag{S2}$$

where I and I_0 are the intensity distributions of diffracted and incident beam, respectively. Equations (S1) and (S2) can be further derived as,

$$I = I_0 (lf'(\theta))^2 / k^4\ , \tag{S3}$$

According to the Eq. (S1), a finite beam radius R implies that the wave vector exists with a minimum boundary, i.e. $k_{min} = lf'(\theta)/R$. For a given azimuth angle, no electrons are diffracted into the range of $k < k_{\min}$, so it would appear as a void region. In the range of $k > k_{\min}$, Eq. (S3) shows that the diffracted intensity I is inversely proportional to the k^4, thus it reaches to a peak at the point of $k_{\min}$ and then decreases sharply with further increase of k. As a result, the local divergence angle of the electron vortex Ω can be defined as the polar angle corresponding to the peak of diffracted intensity, i.e. $\Omega = \arcsin\left(\dfrac{k_{\min}}{k_0}\right) \propto lf'(\theta)$, here k_0 is the wave vector of free-space electron. Therefore, the structured EVB in the far-field will present the same pattern with the curve $f'(\theta)$ in polar coordinates.

Section 2: Fourier series expansion

In this work, the parameterized azimuth gradient plays an important role in determining the pattern of EVB. For the sake of generality, the parameterized azimuth gradient can be written in the form of trigonometric series as

$$f'(\theta) = \alpha\left(a_0 + \sum_{n=1}^{\infty}\left(a_n\cos(n\theta) + b_n\sin(n\theta)\right)\right)\ , \tag{S4}$$

where the scaling factor α is a constant that can be adjusted to satisfy the constraint condition $f(2\pi) - f(0) = 2\pi$. Obviously, any geometry enclosed by a single-value curve $F(\theta)$ in polar coordinates can be used to construct a suitable parameterized azimuth gradient with the relationship of $f'(\theta) = \alpha F(\theta)$, and the corresponding Fourier series expansion coefficients are given as

$$\begin{cases} a_0 = \dfrac{1}{2\pi}\int_0^{2\pi} F(\theta)\,\mathrm{d}\theta \\ a_n = \dfrac{1}{\pi}\int_0^{2\pi} F(\theta)\cos(n\theta)\,\mathrm{d}\theta \\ b_n = \dfrac{1}{\pi}\int_0^{2\pi} F(\theta)\sin(n\theta)\,\mathrm{d}\theta \end{cases} , \tag{S5}$$

The arrowhead contour used in this work is enclosed by a single-value curve $F(\theta)$, as show in Fig. S1(a). Based on the Eqs. (4) and (5), the relevant coefficients in parameterized azimuth gradient $f_3'(\theta)$ are derived as $\alpha = 1$ and $a_0 = 1$. The additional coefficients of the Fourier expansion a_n and b_n are shown in Fig. S1(b). To precisely obtain the arrowhead contour, here we use the first 40 terms of the Fourier expansion.

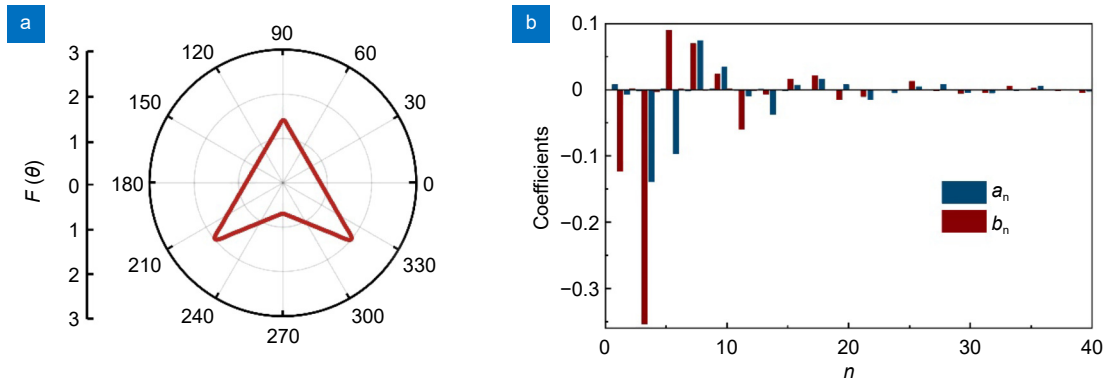

Fig. S1 | (**a**) The arrowhead contour enclosed by a single-value curve in polar coordinates. (**b**) The Fourier series expansion coefficients of the corresponding parameterized azimuth gradient.

Section 3: Design of binary phase mask

In order to produce a structured EVB, the binary phase mask should impart a transverse composite phase profile $\varphi(r,\theta)$, which is the superposition of a generalized spiral phase and a Bragg carrier phase, to the incident electron wave and expressed as:

$$\varphi = \varphi_{\text{spiral}} + \varphi_{\text{Bragg}} = lf(\theta) + \frac{2\pi}{p} r\cos\theta\,, \tag{S6}$$

where l is the topological charge, and p is the carrier period. By performing the binary phase processing of $\varphi(r,\theta)$, the binary phase mask can be constructed with the following shape:

$$H(r,\theta) = \frac{1}{2}H_0\left\{\text{sgn}\left[\cos\left(lf(\theta) + \frac{2\pi}{p}r\cos\theta\right) + D\right] + 1\right\}\,, \tag{S7}$$

where H_0 is the height of holographic grating, sgn is the sign function and D=0.9 is the duty-cycle.

Section 4: Phase retrieval

In order to retrieve the phase profile of the generated EVB, five images (one focal image, two over-focus images and two under-focus images) are experimentally acquired using defocus increments of Δz =2 μm, as shown in Fig. S2. The intensity distribution of each image is I_i ($i = 1 \sim 5$), and thus the amplitude distribution can be expressed as $A_i = \sqrt{I_i}$. We employ defocus series reconstruction technique based on the Gerchberg-Saxton algorithm to iteratively propagate an electron wave between different image planes.

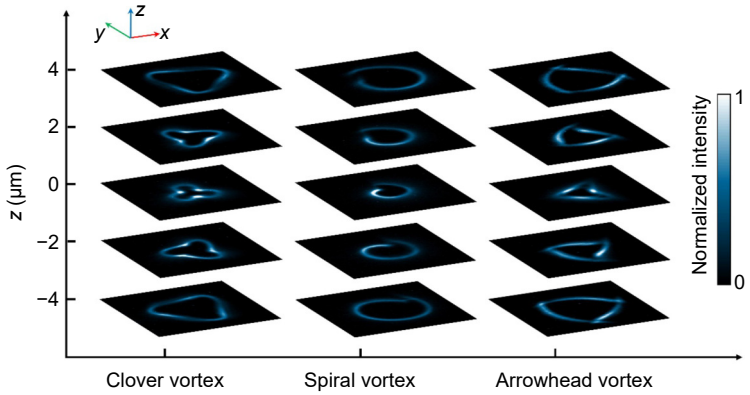

Fig. S2 | Experimentally recorded intensity distributions of the structured EVBs at an interval of 2 μm along the *z* direction. All images have same size of 13.6 μrad × 13.6 μrad.

As shown in flow chart of Fig. S3, the randomly generated phase and the experimentally recorded amplitude A_3 are combined as the wave function at the focal plane (P_3) and begins the initial iteration. By fast Fourier transforming the

product of spectrum and angular spectral transfer function, we can get the wave function at the plane (P_4) as well as the phase distribution. This phase distribution can be used to construct the input wave function for the next iteration by combining the measured amplitude A_4. In the same way, the diffracted electron wave propagating through the five planes forms a loop. We need to replace the amplitude at each plane with the measured value A_i, so that the deviation in the diffraction iteration of the angular spectrum can be corrected. In order to reduce the amount of computation of the Fourier transform while ensuring the recovery accuracy, we set the spatial sampling of each image to 512×512. The recovery quality of the phase can be quantified by calculating the relative mean squared error (RMSE) of two recovered phase distributions,

$$RMSE = \sqrt{\sum_{x=1}^{n_x}\sum_{y=1}^{n_y}\left(\varphi_j\left(x,y\right)-\varphi_{j-1}(x,y)\right)^2 / \sum_{x=1}^{n_x}\sum_{y=1}^{n_y}\left(\varphi_{j-1}\left(x,y\right)\right)^2}\ , \tag{S8}$$

where $\phi_j(x,y)$ and $\phi_{j-1}(x,y)$ are the phase recovered by the jth and $(j-1)$th iterations, respectively. A precise phase distribution can be obtained when RMSE tends to a stable value after hundreds of iterations.

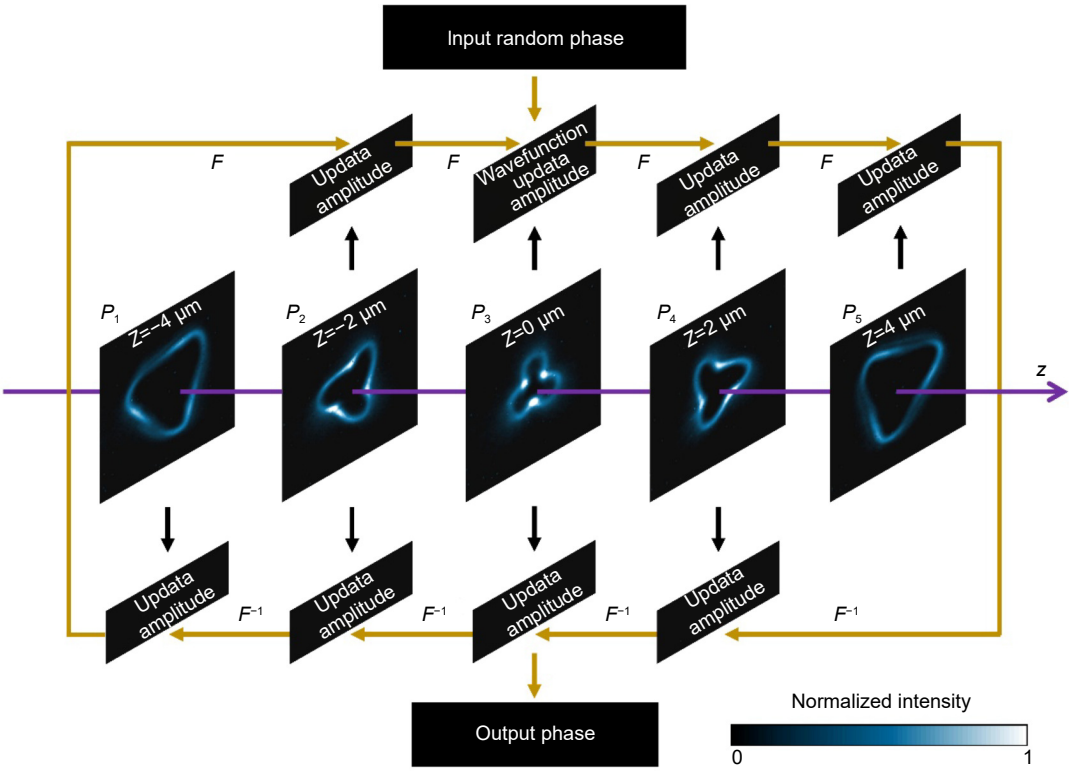

Fig. S3 | Flow chart of electron wavefront retrieval based on the Gerchberg-Saxton transmission iterative algorithm. The symbols *F* and F^{-1} denote the Fourier transform and the inverse Fourier transform, respectively.

Section 5: Modal decomposition

Modal decomposition is an important technique that is often used to quantitatively analyze the OAM spectral distributions of complex beams. As the orbital eigenstates, the wave functions of OAM modes behave as spiral harmonics $\exp(\mathrm{i}l\theta)$ and possess orthogonality properties with respect to each other. Therefore, any complex field can be represented by a linear combination of orthogonal basis modes as,

$$\psi(r,\theta) = \frac{1}{\sqrt{2\pi}}\sum_{l=-\infty}^{+\infty} a_l\left(r\right)\exp\left(\mathrm{i}l\theta\right)\ . \tag{S9}$$

The complex correlation coefficient a_l weights the contribution of l-th OAM mode and can be determined by

$$a(r) = \frac{1}{\sqrt{2\pi}} \int_0^{2\pi} \psi(r,\theta) \left(\exp(il\theta)\right)^* \mathrm{d}\theta \,, \tag{S10}$$

where the asterisk represents the complex conjugate. Thus, the intensity of the l-th OAM mode is,

$$c_l = \int_0^{\infty} |a_l(r)|^2 r \mathrm{d}r \,. \tag{S11}$$

The weight factor of l-th OAM mode is intuitively defined as the relative intensity of such mode, and can be evaluated by normalizing the intensity c_l to the total intensity of the electron beam as,

$$Weightfactor = \frac{c_l}{\sum_{n=-\infty}^{+\infty} c_n} \,. \tag{S12}$$

Based on the above analysis, obviously the OAM spectrum of the complex field can be obtained once we know the wave functions $\psi = A\exp(i\varphi)$. For three structured EVBs demonstrated in this work, the amplitude A is presented as the square root of the experimentally measured intensity distribution, and the phase distribution φ can be obtained through the algorithm iteration described in 'phase retrieval' of methods. The calculated OAM spectral distributions of these three structured EVBs are shown in Fig. 4 in the main text.

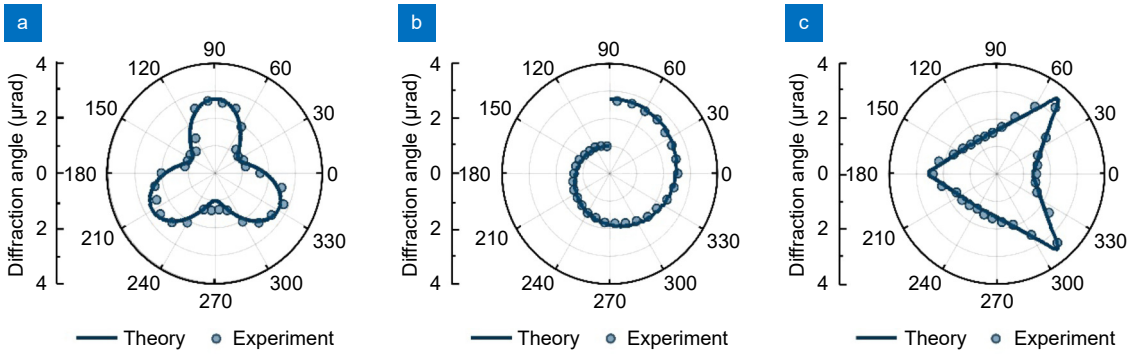

Fig. S4 | (**a**–**c**) Diffraction angle distributions measured along different azimuth angle for three types of structured EVBs with a topological charge l = 30. The measured diffraction angle distributions (blue points) agree well with the theoretical prediction (solid curves).

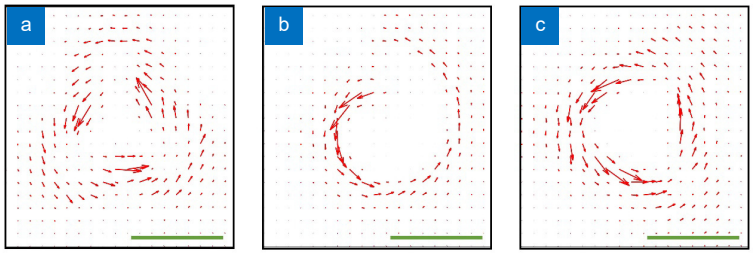

Fig. S5 | (**a**–**c**) The simulated probability current density vector of the three EVBs with topological charge l = 30. The red arrows indicate the direction of the probability current of electron. The length of the red arrows is given in arbitrary unit normalized to the maximum value. Scale bars: 3 μrad. For these EVBs, the calculated average OAM value is 29.91$\hbar$, 29.93$\hbar$ and 29.92$\hbar$, respectively.